ISSN (Print) 1226-1750
ISSN (Online) 2233-6656
Journal of Magnetics 18(3), 302-307 (2013) http://dx.doi.org/10.4283/JMAG.2013.18.3.302

Thrust Hybrid Magnetic Bearing using Axially Magnetized Ring Magnet

Cheol Hoon Park[1,2]*, Sang Kyu Choi[1], Ji Hoon Ahn[1,3], Sang Yong Ham[1], and Soohyun Kim[2]

[1]*Advanced Manufacturing Systems Research Division, Korea Institute of Machinery and Materials, Daejeon 305-343, Korea*
[2]*Department of Mechanical Engineering, Korea Advanced Institute of Science and Technology, Daejeon 305-348, Korea*
[3]*Department of Electrical Engineering, Chungnam National University, Daejeon 305-764, Korea*

(Received 21 June 2013, Received in final form 9 July 2013, Accepted 9 July 2013)

Hybrid-type magnetic bearings using both permanent magnets and electromagnets have been used for rotating machinery. In the case of conventional thrust hybrid magnetic bearings supporting axial loads, radially magnetized permanent ring magnets, which have several demerits such as difficult magnetization and assembly, have been used to generate bias flux. In this study, a novel thrust hybrid magnetic bearing using an axially magnetized permanent ring magnet is presented. Because it is easy to magnetize a ring magnet in the axial direction, the segmentation of the ring magnet for magnetization is not required and the assembly process can be simplified. For verifying the performance of the proposed method, a test rig that consists of a proposed thrust magnetic bearing and variable loads is constructed. This paper presents the detailed design procedures and the obtained experimental results. The results show that the developed thrust magnetic bearing has the potential to replace conventional thrust magnetic bearings.

Keywords : thrust magnetic bearing, ring magnet, axial magnetization

1. Introduction

Recently, magnetic bearings have been extensively used in rotating machinery in the area such as machining tools, flywheel energy storage systems, turbo machinery [1, 2]. In rotating machinery, thrust magnetic bearings support the axial load of the rotor. Thrust magnetic bearings are classified into thrust passive magnetic bearing (thrust PMB), thrust active magnetic bearings (thrust AMB) and thrust hybrid magnetic bearings (thrust HMB). The thrust PMB and AMB generates magnetic flux using permanent magnets (PM) and electromagnets (EM) only, respectively [3-5]. Although the thrust PMB has an advantage of insignificant energy consumption, its insufficient damping is a main drawback. Because the thrust AMB needs to provide bias current continuously to generate bias flux, it also has a drawback that its energy efficiency is not high. On the other hand, the thrust HMB generates magnetic flux by using both an EM and a permanent magnet (PM), and its efficiency is high because bias flux is provided by the PM [6-8]. Lu *et al.* developed an axial actuator based on the theory of the thrust HMB [9]. However, square-shaped permanent magnets were used in it and it generated smaller magnetic force compared to the thrust HMB which used ring-shaped permanent magnet. Han *et al.* and Park *et al.* developed a turbo compressor with a thrust HMB [10, 11]. Although it is advantageous from the viewpoint of energy efficiency, this thrust HMB is equipped with a radially magnetized ring magnet (thrust RM-HMB). In the case of ring magnets, it is hard to magnetize in the radial direction, and segmentation is required for magnetization. This makes the assembly process difficult. If it is possible to use an axially magnetized ring magnet in a thrust HMB, these problems can be solved. The purpose of this paper is to present the design procedure of the thrust HMB using an axially magnetized ring magnet (thrust AM-HMB) and the experimental results. This will help in simplifying the assembly process of the thrust HMB.

2. Configuration of Thrust RM-HMB

A detailed configuration of the thrust RM-HMB is shown in Fig. 1. The magnetic flux paths from the radially magnetized ring magnet (red arrow line) and electromagnet (blue arrow line) are shown, as well. Because

*Corresponding author: Tel: +82-42-868-7980
Fax: +82-42-868-7135, e-mail: parkch@kimm.re.kr

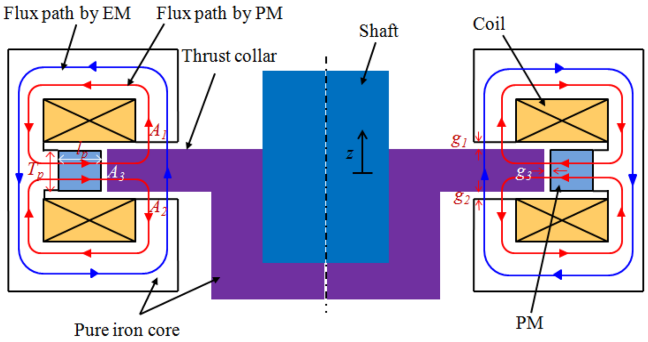

Fig. 1. (Color online) Configuration and magnetic flux paths of thrust RM-HMB.

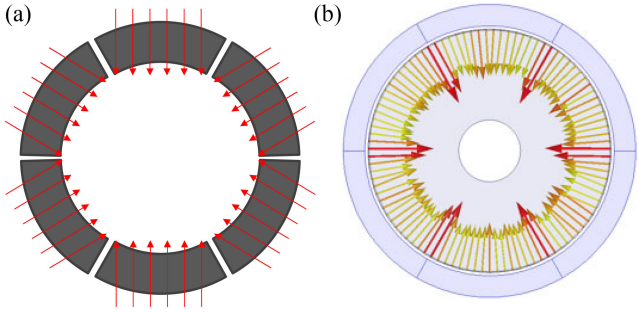

Fig. 3. (Color online) (a) Assembled ring magnet after parallel magnetization and (b) non-uniform magnetic flux at boundaries of segments.

the ring magnet is magnetized in the radial direction, the flux path from the PM is symmetric with respect to the center line of the upper and lower sides of the pure iron core. The magnetic flux from the PM provides bias flux to the upper and lower gaps (g_1 and g_2) between the thrust collar and the pole face of the pure iron core. Axial force in the thrust RM-HMB can be dynamically controlled by changing the amount of current flowing into the serially connected ring coil. However, there are several problems in the manufacturing and assembly processes of radially magnetized ring magnets. Figure 2 shows the manufacturing procedure of a radially magnetized ring magnet. Because it is almost impossible to magnetize the entire ring magnet in the radial direction, in practice, a ring magnet is segmented into 6 or 8 pieces, and each segment is separately magnetized in the radial direction. One of the problems with a segmented ring magnet is that it is not easy to assemble all the pieces of the magnet into one ring magnet again and control the gap between the magnet and the thrust collar. Another problem is that the radial magnetic flux becomes non-uniform on the boundaries of the segmented magnets as shown in Fig. 3, which results in performance degradation.

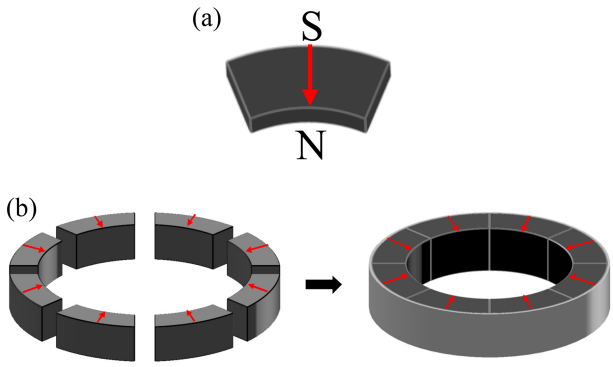

Fig. 2. (Color online) Manufacturing procedure of radially magnetized ring magnet: (a) parallel magnetization for each segment. (b) assembly of all segments into ring frame.

3. Thrust HMB with Axially Magnetized Ring Magnet

An axially magnetized ring magnet is shown in Fig. 4. Because it is easy to magnetize the ring magnet in the axial direction, the segmentation of the ring magnet for magnetization is not required and the assembly process can be simplified. In order to solve the abovementioned problems, a thrust AM-HMB was designed as shown in Fig. 5 by using this axially magnetized ring magnet. In

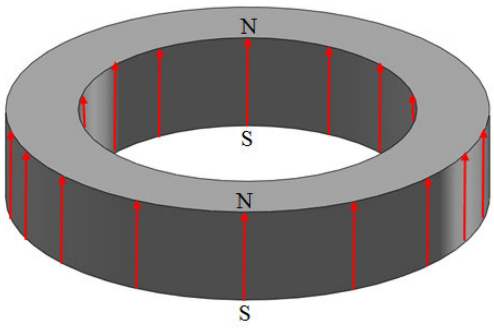

Fig. 4. (Color online) Axially magnetized ring magnet.

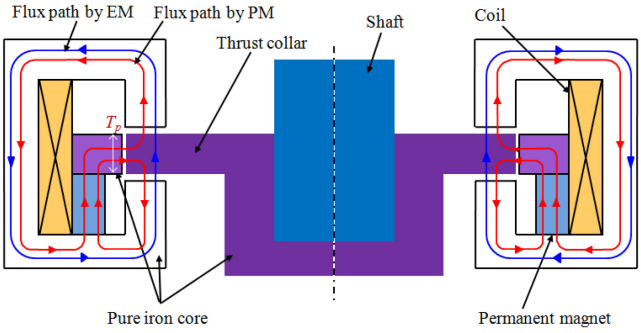

Fig. 5. (Color online) Configuration and magnetic flux paths of thrust AM-HMB.

order to assemble the thrust AM-HMB, the ring coil is first installed inside of the pure iron core. Then, the stack of the axially magnetized ring magnet and pure iron ring is installed inside of the ring coil.

The magnetic flux from the ring magnet in the thrust RM-HMB has paths that go through the thrust collar and pure iron stator. Similarly, in case of the thrust AM-HMB, the magnetic flux from the ring magnet has a path that goes through the pure iron ring, thrust collar, and pure iron stator. As a result, the axially magnetized ring magnet could also provide bias flux to the upper and lower gaps in the same manner as the radially magnetized ring magnet.

Because the configuration of the thrust AM-HMB is similar to the thrust RM-HMB, the design procedures are almost the same. In order to design the thrust RM-HMB shown in Fig. 1, $\phi_{PM\,up}$, the magnetic flux in the air gap, g_1, which is induced by the PM, can be given by

$$\phi_{PM\,up} = \frac{l_p H_c}{\frac{g_1}{\mu_0 A_1} + \frac{g_3}{\mu_0 \frac{A_3}{2}} + \frac{l_i}{\mu_0 \mu_i A_i} + \frac{l_p}{\mu_0 \mu_p \frac{A_p}{2}}} \tag{1}$$

where l_i is the length of the flux path in pure iron core, l_p is the radial length of the PM, H_c is the coercivity of the PM, μ_0 is the magnetic permeability of free space, μ_p is the relative magnetic permeability of the PM, μ_i is the relative magnetic permeability of the pure iron core, g_1 is the air gap length between the upper pole face and the thrust collar, g_3 is the air gap length between the outer side of the thrust collar and the inner side of the PM, A_1 is the area of the upper pole face, A_3 is the area of the air gap between the inner area of the PM and the outer area of the thrust collar, A_i is the effective area of the pure iron core, and A_p is the effective area of the PM. After magnetic flux from the PM passes through A_3, it splits into two paths and passes through A_1 and A_2. Only the magnetic flux induced by the PM passes through A_3, whereas the magnetic flux induced by both PM and EM pass through A_1 and A_2. Therefore, it is appropriate to select A_3 to be the same as A_1 ($A_1 = A_3$). If the magnetic reluctance of the pure iron core is neglected, and we assume $A_1 = A_3 = A$, Eq. (1) can be written as Eq. (2).

$$\phi_{PM\,up} = \frac{l_p H_c}{\frac{g_1}{\mu_0 A} + \frac{g_3}{\mu_0 \frac{A}{2}} + \frac{l_p}{\mu_0 \mu_p \frac{\gamma A}{2}}} \tag{2}$$

where γ is the ratio of A_p to A_3. The magnetic flux in the air gap between the upper pole face and the thrust collar that is induced by the EM, $\phi_{EM\,up}$, is given by Eq. (3).

$$\phi_{EM\,up} = \frac{2\mu_0 ANi}{g_1 + g_2} = \frac{\mu_0 ANi}{g_0} \tag{3}$$

where g_0 is a nominal gap, N is the number of coil turns per pole, and i is the current to the EM. If the vertical displacement of the shaft is z, then $g_1 = g_0 - z$ and $g_2 = g_0 + z$. Assuming γ is 1, flux density B_{up} and generated force F_{up} in air gap g_1 can be written as Eqs. (4) and (5), respectively.

$$B_{up} = \frac{\phi_{PM\,up} + \phi_{EM\,up}}{A} = \frac{\mu_0 l_p H_c}{g_1 + 2g_3 + \frac{2l_p}{\mu_p}} + \frac{\mu_0 Ni}{g_0} \tag{4}$$

$$F_{up} = \frac{B_{up}^2}{2\mu_0} A = \frac{\mu_0 A}{2}\left(\frac{l_p H_c}{g_1 + 2g_3 + \frac{2l_p}{\mu_p}} + \frac{Ni}{g_0}\right)^2 \tag{5}$$

In a manner similar to that of Eqs. (1)-(5), generated force F_{down} in air gap g_2 can be written as Eq. (6).

$$F_{down} = \frac{B_{down}^2}{2\mu_0} A = \frac{\mu_0 A}{2}\left(\frac{l_p H_c}{g_1 + 2g_3 + \frac{2l_p}{\mu_p}} - \frac{Ni}{g_0}\right)^2 \tag{6}$$

From Eqs. (5) and (6), the net force acting on the thrust collar from the thrust RM-HMB is given by

$$F_{net} = F_{up} - F_{down} = \frac{\mu_0 A}{2}\left(\left(\frac{l_p H_c}{(g_0 - z) + 2g_3 + \frac{2l_p}{\mu_p}} + \frac{Ni}{g_0}\right)^2 - \left(\frac{l_p H_c}{(g_0 + z) + 2g_3 + \frac{2l_p}{\mu_p}} - \frac{Ni}{g_0}\right)^2\right) \tag{7}$$

In Eq. (7), the design parameters for the thrust RM-HMB are l_p, H_c, N, A, g_0, and g_3. Except for l_p, the design parameters for the thrust AM-HMB are the same as those of the thrust RM-HMB. If l_p is replaced by T_p, Eq. (7) becomes the net force on the thrust collar from the thrust AM-HMB. If T_p of the thrust AM-HMB is selected to be the same value as l_p of the thrust RM-HMB, the net force becomes the same for both types of thrust HMB.

4. Prediction of Leakage Flux by Considering Fringing Effect

Although the proposed magnetic bearing has fringing effect in air-gap, Eqs. (1)-(7) do not consider fringing effect. However, it should be considered in the analysis to improve the accuracy, and the procedure to obtain the

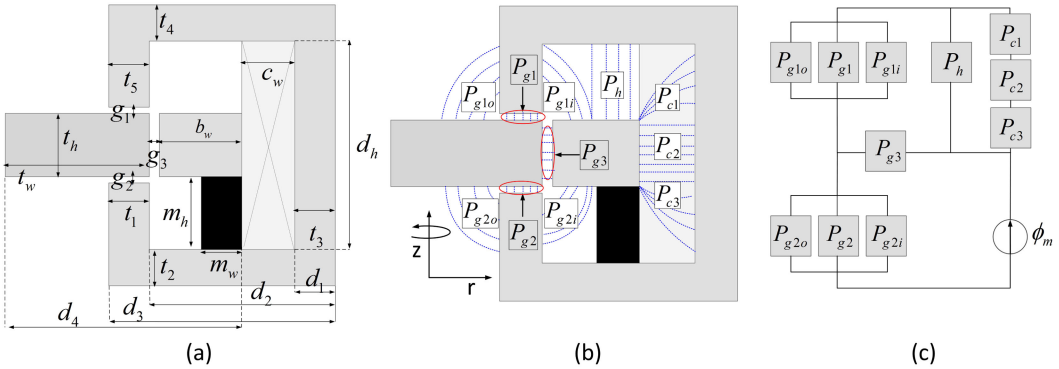

Fig. 6. (Color online) (a) Analysis model of thrust AM-HMB, (b) fringing flux at an air gap and (c) EMC considering fringing effect.

permeance considering fringing effect is described in this chaper [12, 13]. There is a method to analyze the static characteristics of magnetic bearings: by using the equation for thrust obtained from the equivalent magnetic circuit (EMC), and if these fringing effects are included, an accurate EMC could possibly be obtained. Figure 6(a) illustrates analysis model of AM-HMB. The fringing effect should be considered as shown in Fig. 6(b) to calculate thrust accurately, and an EMC considering the fringing effect was constructed as shown in Fig. 6(c).

Flux lines spreading out into the air in Fig. 6(b) describe the fringing flux. The permeance relating to the fringing flux in the air gap can be separated into the components P_g, P_c, and P_h as follows [12]:

$$P_{g1} = \frac{\mu_0 A_1}{g_1} \tag{8a}$$

$$P_{g2} = \frac{\mu_0 A_2}{g_2} \tag{8b}$$

$$P_{g3} = \frac{\mu_0 A_3}{g_3} \tag{8c}$$

$$P_h = \frac{\mu_0 S_m}{g_h} \tag{8d}$$

$$P_{c1} = \frac{\mu_0 d_4^2 \pi^3 c_w}{4}\left(\frac{1}{1.211 c_w}\right)^2 = P_{c3} \tag{8e}$$

$$P_{c2} = \frac{\mu_0 2\pi d_1\left(d_h - \frac{3}{5}c_w\right)}{c_w} \tag{8f}$$

$$P_{g1i} = 8\mu_0\left[d_2\left\{\ln\left(g_{1i} + d_h + \frac{3}{10\pi c_w}\right)\right\} + d_3\left\{\ln\left(g_{1i} + t_h + \frac{3}{9\pi m_w}\right)\right\} - 2\ln(g_{1i} + t_h)\right] \tag{8g}$$

$$P_{g2i} = 8\mu_0 d_3\left[\ln\left(g_{2i} + m_h + \frac{1}{9\pi m_w}\right) - \ln(g_{2i} + m_w)\right] \tag{8h}$$

$$P_{g1o} = 8\mu_0 d_4\left[\ln\left\{g_{1o} + (t_w - t_5) + \frac{1}{7\pi m_w} + \frac{3}{10\pi c_w}\right\} - \ln(g_{1o} + t_h)\right] \tag{8i}$$

$$P_{g2o} = 8\mu_0 d_4\left[\ln\left\{g_{2o} + (t_w - t_i) + \frac{1}{7\pi m_w}\right\} - \ln(g_{2o} + t_h)\right] \tag{8j}$$

Here, each g is the length of the air gap; d_h is the length of pure-iron core; c_w is the wide of coil area; m_w and m_h are the wide of PM and the height of PM, respectively; t_w is the length of thrust collar. Therefore, the composite permeance of the air gap can be described as Eqs. (9a)-(9c), and the prediction of the generating force can be improved by applying them into Eqs. (1)-(3).

$$P_c = P_{c1} + P_{c2} + P_{c3} \tag{9a}$$

$$P_{g1}' = 1/\left(\frac{1}{P_{g1o}} + \frac{1}{P_{g1}} + \frac{1}{P_{g1i}}\right) \tag{9b}$$

$$P_{g2}' = 1/\left(\frac{1}{P_{g3o}} + \frac{1}{P_{g3}} + \frac{1}{P_{g3i}}\right) \tag{9c}$$

5. Experimental Verification of Thrust AM-HMB

A test rig was designed to verify the design concept of the thrust AM-HMB. The axial load to be supported by the thrust AM-HMB was selected to be ranging from –2,000 to 2,000 N. First, the design parameters of the thrust RM-HMB were selected by referring to Eqs. (1)-(7). Second, the thickness of the ring magnet for the thrust AM-HMB was selected to be l_p of the designed thrust RM-HMB. Table 1 shows the specifications of the

Table 1. Specifications of the thrust AM-HMB for test rig.

Item	Specifications
Load capacity [N]	–2,000-2,000
Current range [A]	–7-7
Nominal gap, g_0 [mm]	0.6
Area of pole face, A [m^3]	4.04e-3
Air gap, g_3 [mm]	1
Number of coil turns	80
Inner diameter of ring magnet [mm]	114
Outer diameter of ring magnet [mm]	130
Magnet	NdFeB (N42H)

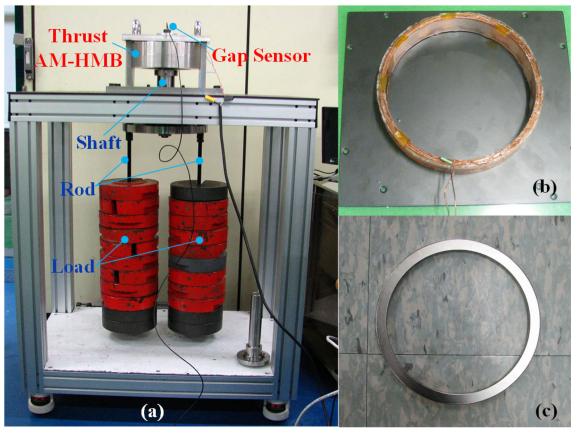

Fig. 7. (Color online) Test rig for thrust AM-HMB: (a) fabricated test rig under load. (b) coil. (c) axially magnetized ring magnet.

designed thrust AM-HMB. It should be noted that the number of turns in Table 1 is double the value of N in Eq. (7) because in the thrust RM-HMB, two ring coils, each with N turns, are serially connected, whereas one ring-shaped coil with 2 N turns is used in the thrust AM-HMB. Finally, leakage flux component were considered for accurate analysis considering fringing effect.

Figure 7 shows the designed and fabricated test rig for the thrust AM-HMB. The shaft and rods to add loads are attached to the thrust collar. A gap sensor measures the vertical displacement of the thrust collar, and the current to the electromagnet is adjusted by a controller to maintain the gap between the thrust collar and the pole faces. When the load is added to the thrust AM-HMB, the current increases to generate an upward magnetic force and maintain the gap. Figure 8 shows the relationship between the load and the current in the thrust AM-HMB. Analytical results using Eq. (7) with Eq. (8a)-(9c) and the FE analysis results supported a similar prediction, that the thrust AM-HMB would support about 1,900 N with a current of 7 A. From the experiment, it was found that the

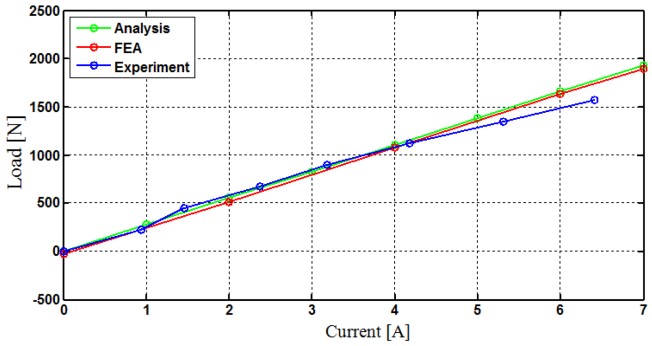

Fig. 8. (Color online) Relationship between load and current in thrust AM-HMB.

fabricated thrust AM-HMB showed a similar load capacity as the prediction, although the magnetic force became somewhat saturated when the current exceeded 5 A.

6. Conclusion

This paper presented the design procedure of a thrust hybrid magnetic bearing using an axially magnetized ring magnet and the experimental results. It was found that the fabricated thrust magnetic bearing could support a load in the range 0-160 kg with a current in the range 0-6.5 A. Because the experimental results show good agreement with the simulation results, it is possible to say that the design procedure for the axially magnetized thrust hybrid magnetic bearing is reliable. This new type of thrust magnetic bearing could be extensively applied to rotating machinery and would help simplify the assembly of thrust hybrid magnetic bearings.

References

[1] C. R. Knospe, Control Eng. Pract. **15**, 307 (2007).
[2] G. Schweitzer, "Applications and research topics for active magnetic bearings," IUTAM Symp. Emerging Trends in Rotor Dynamics, Springer Netherlands, 2011.
[3] J. Fang, Y. Le, J. Sun, and K. Wang, IEEE Trans. Magn. **48**, 2528 (2012).
[4] P. E. Allaire, A. Mikula, B. B. Banerjee, D. W. Lewis, and J. Imlach, J. Franklin Inst. **326**, 831 (1989).
[5] D. O. Baun, R. L. Fittro, and E. H. Maslen, J. Eng. Gas Turbine Power. **119**, 942 (1996).
[6] E. H. Maslen, P. E. Allaire, M. D. Noh, and C. K. Sortore, J. Tribol. **118**, 839 (1996).
[7] Y. H. Fan and A. C. Lee, J. Franklin Inst. **334**, 337 (1997).
[8] J. Fang, J. Sun, and J. Tang, IEEE Trans. Magn. **46**, 4034 (2010).
[9] X. D. Lu and D. L. Trumper, Annals of CIRO. **54**, 383

(2005).
[10] D. C. Han, I. B. Chang, I. H. Park, and Y. H. Park, US Patent 2009/0072644 A1, 2009.
[11] C. H. Park, S. K. Choi, and S. Y. Ham, Proceeding of 2011 IEEE Conference on Automation Science and Engineering. (2011) pp. 792-797.
[12] S. M. Jang, K. H. Kim, K. J. Ko, J. H. Choi, and S. Y. Sung, J. Appl. Phys. **111**, 07E726 (2012).
[13] E. Hou and K. Liu, IEEE Trans. Magn. **47**, 4725 (2011).